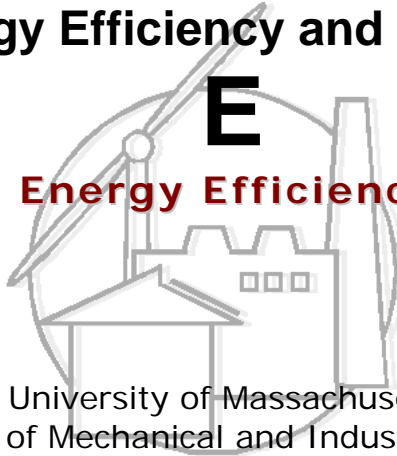


Center for Energy Efficiency and Renewable Energy

C E E R E

Building Energy Efficiency Program



University of Massachusetts
Department of Mechanical and Industrial Engineering
160 Governor's Dr.
Amherst, MA 01003-9265

Progress Report

Laminar Natural Convective Flow in Inclined Rectangular Glazing Cavities

Yunhua Yang

January, 2002

1 Introduction

The importance of natural convective heat flow in a confined cavity is already presented in a lot of literature reviews. One of the most important applications is the building components, such as unventilated walls, double-glazed windows, etc. Though a number of numerical and experimental research work has been done on this topic, these work mostly focus on cavities relatively short compared to glazing cavities. In addition, most of the work only studied the case that cavities are located at vertical orientation.

In this study, natural convection in inclined rectangular glazing cavities is studied numerically by finite element method. Basically speaking, 2-D numerical model provided heat transfer results, with which general heat transfer correlation could be developed for engineering applications such as design, as rough directions. However, because of the three-dimensionality of the flow characteristics, detailed heat transfer results will have to rely on 3-D numerical simulations.

2 Review of the Problem

The geometry and the perfect boundary conditions for the glazing cavity at a tilt orientation are shown in Figure 1, where the Cartesian coordinate system is rotated with the cavity. The angle made by the horizontal line and the cavity hot sidewall is referred to as the tilt angle α . When treating the problem in 2-D, it could be assumed that the cavity is infinitely long in z -direction. The two sidewalls are held at constant temperatures T_1 and T_0 with $T_1 > T_0$. The top and bottom walls are adiabatic (zero heat flux).

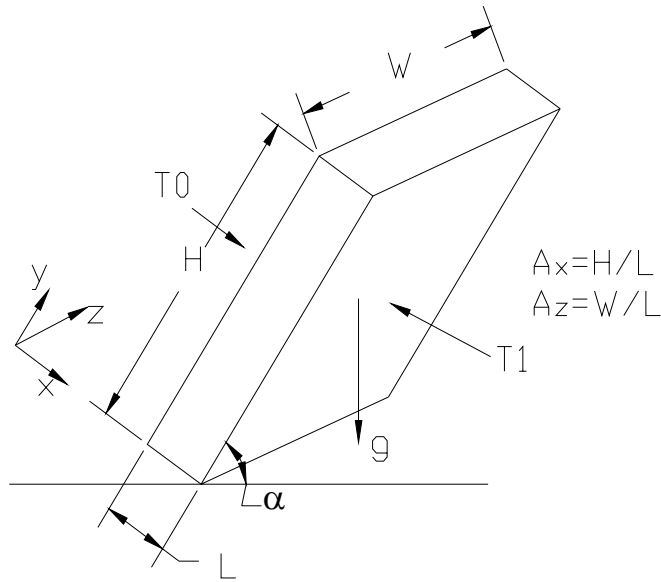


Figure 1: Geometry and Perfect Boundary Condition of the inclined cavity model

Hollands and Konicek (1973) studied the critical Ra number at horizontal, vertical and inclined orientations using a cavity with an aspect ratio 44, and the principal modes of flow were discussed for inclined orientations. For the inclined cases, two types of instabilities should be considered, the static top-heavy associated with the horizontal case and the gravitational buoyancy associated with the vertical case. The relative magnitude of the influence of each depends on the angle of inclination, and at the critical angle heat transfer changes from one mode to the other mode, and the type of flow is roll-like with axis in the y-direction below the critical angle and in the z-direction beyond the critical angle. The heat transfer rate decreases monotonically with increasing angle of inclination up to 90° for Rayleigh numbers slightly higher than the critical Rayleigh number.

Elsherbiny et al. (1982) conducted a study on six aspect ratios between 5 and 110 and Ra number in the range of 10^2 to 2×10^7 to examine the influence of the angle of inclination and the aspect ratio on the heat transfer rate and developed a correlation for

60°. They also suggested a straight line interpolation between 60° and 90° for the range of 60° to 90°.

In a series of papers Ozoe et al. 1974a, 1974b, 1975 and 1983, experimental and numerical studies were carried out in inclined cavities with small aspect ratios (up to 15.5). Their studies provided that the transition angle, where the flow changes its roll patterns, are associated with the local minimum heat transfer rate between 0° and 90°, which are two local maximum points. They also reported that the angle of inclination at the critical conditions is a strong function of the aspect ratio and a weak function of the Ra number. A series of oblique rolls with their axes parallel to the upslope plane but not parallel to each other was first observed from this work.

In Ozoe et.al. (1983) three-dimensional finite-difference method was used to study a rectangular inclined cavity. As shown photographically by Ozoe et.al. (1977), inside the inclined cavity, there are a series of 3-D rolls aligned along z-direction, and the rolls have oblique axis which has some deflection to the y-direction. However, each of these rolls is confined to a rectangular volume, hereafter designated as a cell, whose dimensions do not change with inclination, i.e. each fluid particle remains within the cell. It is this observation that makes the model possible. In their study, a cavity with length =1, Height =7 and width =10 was divided to several rectangular cells with a length-to-height ratio of 7 and several postulated width-to-height ratios near unity. The 3-D velocity and temperature fields and in turn, the average Nusselt number and representative streaklines were computed for the typical cell.

Arnold et al. (1976) experimentally investigated steady natural convection heat transfer in inclined rectangular cavities with 4 aspect ratios of 1, 3, 6, and 12, and Ra

number up to 10^6 . They also observed the minimum heat transfer between horizontal and vertical orientations associated with the transition of the flow motions. The results also indicate that the transition between the two motions changes for differing aspect ratios. The minimum occurred at 70° for aspect ratio 12, and as the aspect ratio is decreased, the angle at which the minimum occurred decreased towards 0° . They determined that the occurrence of a minimum shows that the two forms of motion do not superimpose; rather one or the other prevails. In general, their results showed reasonable agreement with those of Ozoe et al (1975).

Schinkel and Hoogendorn (1978) performed an interferometric study on the local heat transfer by natural convection in inclined enclosures. The range of the aspect ratio they studied was between 27 and 6 and Ra number up to 4×10^6 . They reported that the average Nu number monotonously increases with decreasing angle of inclination. Their explanation for this phenomena is that, the aspect ratio is 27 in their experiments at $Ra < 10^5$ and 6 at $Ra \cong 10^6$, so at low Ra number the aspect ratio is too large to observe a minimum while at small aspect ratios the Ra number is too high to observe this effect.

Linthorst et al. (1981) carried out flow visualization experiments to study the flow structure with natural convection in inclined enclosures. Observations were made for aspect ratio 0.25 to 7, angles of inclination from 0° to 90° and Ra number between 5×10^3 and 2.5×10^5 . They reported that the transition from stationary two-dimensional to stationary three-dimensional flow occurs with increasing aspect ratio for increasing angles of inclination for aspect ratio larger than 1. And the angle of flow mode transition is only slightly dependent only on Ra number. This is in agreement with experiments of Ozoe et al (1975).

Hamady et al. (1989) obtained measurements of local and mean Nu numbers at inclined angles for Ra number between 10^4 and 10^6 and compared their experimental data to the numerical data. Their aspect ratio A is 1 and A_z is 10. Their experimental results showed that the heat transfer rate continues to increase from 180° (heated from up) until a maximum value is reached at an angle between 70° and 60° . Below this point a decrease in angle will result in a decrease of the average heat transfer until a local minimum between 30° and 20° . Then the heat transfer increased reaching a weak maximum value at 0° . The minimum occurs when the flow exhibits a transition from longitudinal rolls to a three-dimensional cellular flow configuration. Their 2-D numerical results showed good agreement with the experimental data beyond 30° . The numerical scheme became unstable at an inclination angle smaller than 30° . Similarly, the instability in the numerical schemes below 30° is reported by Catton et al. (1974).

In the recent paper of Soong, et al. (1996), cavities with aspect ratio 4, 3 and 1 were studied. The results showed that, for a certain aspect ratio, the transition point of the flow mode moves to high angle of inclination as the Rayleigh number increases. And hysteresis phenomena were demonstrated for $Ra \geq 2000$. The same model of square enclosure from Ozoe, et al. (1974a) was studied with the imperfect constant wall temperature boundary conditions, and the results showed good agreement with the experimental curve. Thus, it was believed that effect of the imperfect thermal boundary conditions in the experimental setup was one of the possible reasons to account for the inconsistency of the predictions between the experiments and numerical studies.

Chen and Talaie (1985) carried out a numerical study on laminar natural convection in 2-D inclined rectangular enclosures. The range of parameter considered

are $10^3 \leq Gr \leq 10^7$, $1 \leq A \leq 10$ and $Pr = 1$ and 10 . The effect of inclination angle on average Nusselt Number is such that by decreasing the inclination angle from 90° to 0° , it first increases but then decreases after reaching a peak. The peak of the average Nusselt Number depends on the Grashof Number.

Based on the discussions above, it can be inferred that the flow in the enclosure is quite complex. It is basically three-dimensional. However, it is interesting to see that some researcher can tackle this problem with 2-D model, with quite some success. In this research, the computing resource available is limited, and this is the case with most of the designers, therefore, 2-D model was utilized in this research to study to what extent 2-D model can be applied to analyze the fluid flow and heat transfer in an inclined cavity.

3. 2-D Mathematical Models

For calculation purposes, it is convenient to non-dimensionalize the governing equations and to introduce the characteristic dimensionless numbers. The governing equations are non-dimensionalized using the following relations and scaling quantities:

$$u^* = \frac{u}{U}, \quad v^* = \frac{v}{U}, \quad U = \frac{\alpha}{L} \sqrt{Ra Pr} = \sqrt{g \beta \Delta T L}$$

$$x^* = \frac{x}{L}, \quad y^* = \frac{y}{L}$$

$$\theta^* = \frac{T - T_0}{\Delta T}, \quad \Delta T = T_H - T_C$$

$$p^* = \frac{pL}{\mu U}$$

$$Ra = \frac{\rho g \beta (T_H - T_C) L^3}{\mu \alpha}, \quad Pr = \frac{\nu}{\alpha} = \frac{\mu C_p}{k}$$

$$t^* = \frac{tU}{L}$$

The Boussinesq approximation as well as the assumption of an incompressible fluid flow are applied. The Governing equations in non-dimensional form are:

$$\text{Continuity equation: } \frac{\partial u^*}{\partial x^*} + \frac{\partial v^*}{\partial y^*} = 0 \quad (1)$$

Momentum equations:

x-direction:

$$\sqrt{\frac{Ra}{Pr}} \left[\frac{\partial u^*}{\partial t^*} + u^* \frac{\partial u^*}{\partial x^*} + v^* \frac{\partial u^*}{\partial y^*} \right] = -\frac{\partial p^*}{\partial x^*} + \left[\frac{\partial^2 u^*}{\partial x^{*2}} + \frac{\partial^2 u^*}{\partial y^{*2}} \right] - \sqrt{\frac{Ra}{Pr}} \theta^* \cos \alpha \quad (2)$$

y-direction:

$$\sqrt{\frac{Ra}{Pr}} \left[\frac{\partial v^*}{\partial t^*} + u^* \frac{\partial v^*}{\partial x^*} + v^* \frac{\partial v^*}{\partial y^*} \right] = -\frac{\partial p^*}{\partial y^*} + \left[\frac{\partial^2 v^*}{\partial x^{*2}} + \frac{\partial^2 v^*}{\partial y^{*2}} \right] + \sqrt{\frac{Ra}{Pr}} \theta^* \sin \alpha \quad (3)$$

Energy equation:

$$\sqrt{Ra Pr} \left[\frac{\partial \theta^*}{\partial t^*} + u^* \frac{\partial \theta^*}{\partial x^*} + v^* \frac{\partial \theta^*}{\partial y^*} \right] = \frac{\partial^2 \theta^*}{\partial x^{*2}} + \frac{\partial^2 \theta^*}{\partial y^{*2}} \quad (4)$$

The boundary conditions imposed in the dimensionless form for this problem are as follows:

Temperature boundary conditions on the side walls:

$$\theta^*(x^* = 0, y^*) = 0, \quad \theta^*(x^* = 1, y^*) = 1 \quad (5)$$

Non-slip velocity boundary conditions on all bounding surfaces are:

$$u^*(x^* = 0, y^*) = v^*(x^* = 0, y^*) = 0 \quad (6)$$

$$u^*(x^* = 1, y^*) = v^*(x^* = 1, y^*) = 0 \quad (7)$$

$$u^*(x^*, y^* = 0) = v^*(x^*, y^* = 0) = 0 \quad (8)$$

$$u^*(x^*, y^* = H^*) = v^*(x^*, y^* = H^*) = 0 \quad (9)$$

where H^* is the dimensionless height of the cavity.

Boundary conditions at the top and bottom surfaces:

$$\text{ZHF: } \left. \frac{\partial \theta^*}{\partial y^*} \right|_{y^*=0} = 0, \quad \left. \frac{\partial \theta^*}{\partial y^*} \right|_{y^*=H^*} = 0 \quad (10)$$

The dimensionless parameters governing the flow behavior in a vertical IGU cavity are, aspect ratio A and Rayleigh number Ra .

The aspect ratio A is defined by,

$$A = \frac{H}{L} \quad (11)$$

where H is the height of the cavity and L is the length of the cavity.

4. Results

4.1 Comparison to published experimental work

4.1.1 $Ra=6559.7$, $A=38.25$ (Cavity 1 from the seven IGU)

Figure 2 represents the average Nusselt number corresponding to different angle of inclinations. The results from current study are represented by Fidap-2D in the Figure 2. Figure 3 shows the cell patterns inside the cavity at some selected angles.

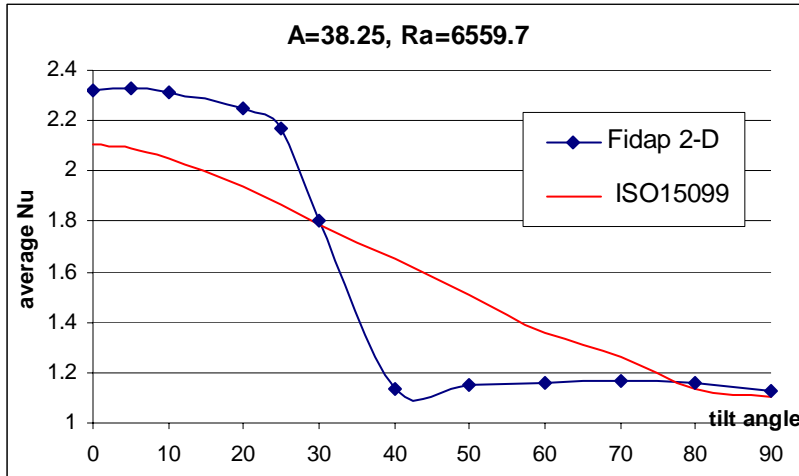


Figure 1: Average Nusselt number from tilt angle 0° to 90° for A=38.25, Ra=6559.7.

Generally speaking, Fidap 2-D model does not present a perfect match between its results and those publicly accepted. Except at $\theta = 30^\circ$, 80° and 90° , there is apparent discrepancy between the two results. The maximal magnitude of relative error occurs at around $\theta = 40^\circ$, with the error mounts up to 30 percent, which, however, is still acceptable for a lot of design purposes. The discrepancy is believed to be caused by many factors, among which three-dimensionality of the flow and imperfect boundary condition are the two most important ones. Their influence, especially of the latter, will be discussed in the later part of this report. Another point worth mentioning is that ISO 15099 presents a monotonically decreasing curve, whereas a local weak minimum can be found in the Fidap 2-D model.

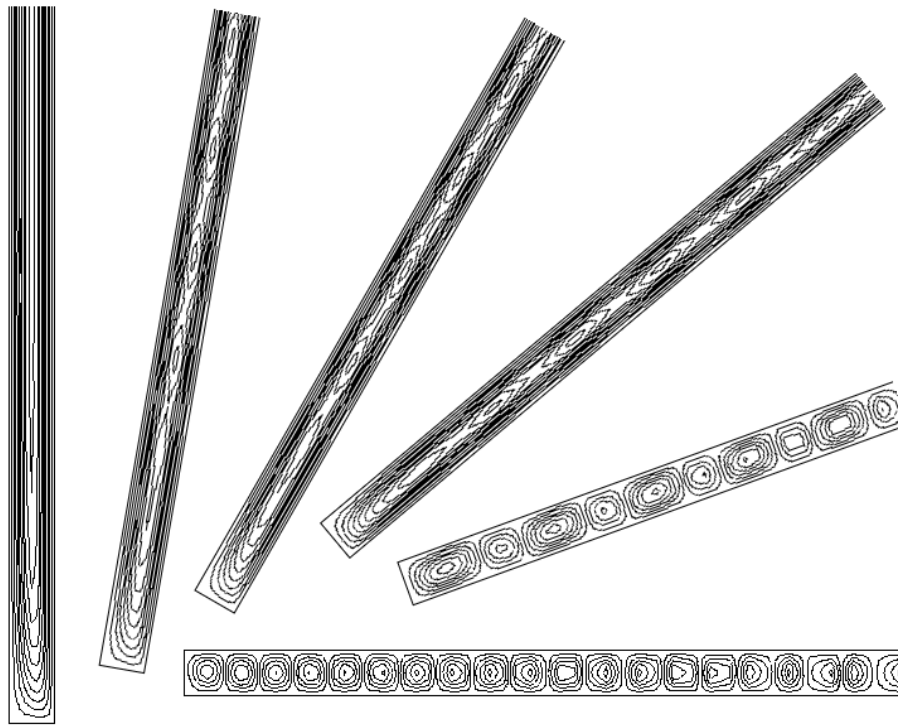


Figure 2: Streamline contours in the cavity at selected tilt angles (only 1/3 of the total height from the bottom). From left to right list tilt angles 90° , 80° , 60° , 40° , 20° , 0° .

4.1.2 $Ra=3760$, $A=15.5$

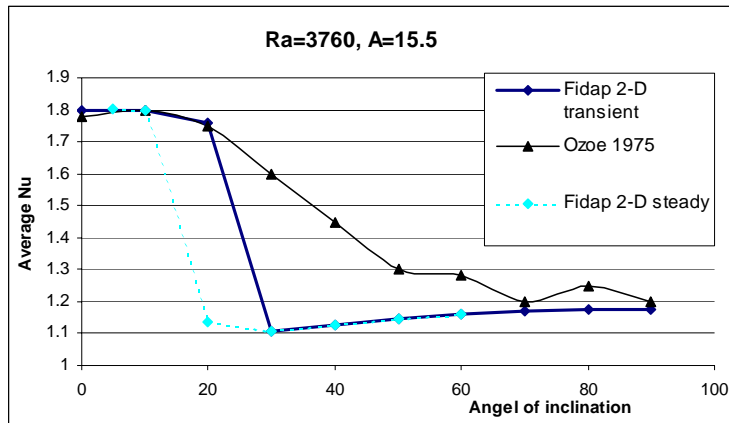


Figure 4: Average Nusselt number from tilt angle 0° to 90° for $A=15.5$, $Ra=3760$.

Figure 4 represents the average Nusselt number corresponding to different angles of inclination together with the experimental data from Ozoe (1975) for the same aspect ratio $A=15.5$ and $A_z=15.5$ (the ratio of the depth in z-direction over the width in x-direction) and the same Rayleigh number. Again, obvious discrepancy is found for θ between 30° and 70° , with the maximum magnitude of relative error of around 30% at $\theta = 30^\circ$. Two models, one transient and the other steady state, were used for this case. It is interesting to find that steady state and transient model give almost the same results at high tilt angle, while there is a large difference between the two results at $\theta = 20^\circ$. It is believed by the author that this phenomenon is related with the transient nature of the flow around the critical angle, although the critical angle was not predicted correctly using the 2-D model.

4.1.3 $Ra=110,000$, $A=1$

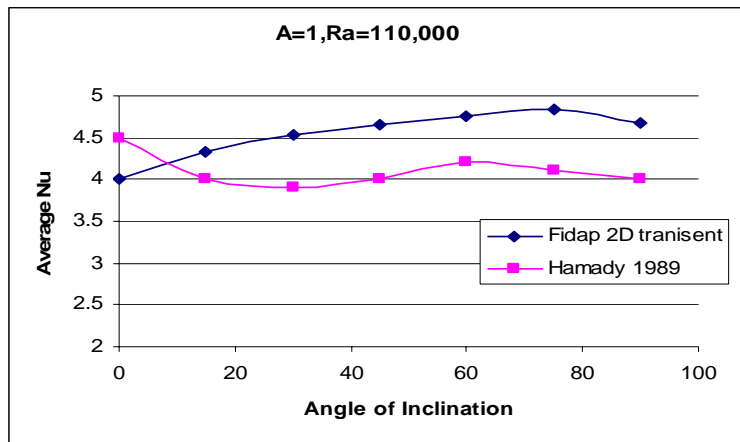


Figure 5: Average Nusselt number from tilt angle 0° to 90° for $A=1$, $Ra=110000$.

Figure 5 represents the average Nusselt number corresponding to different angle of inclinations compared to the experimental data from Hamady (1989) with the aspect ratio $A=1$ and $A_z=10$ (the ratio of the depth in z-direction over the width in x-direction)

and the same Rayleigh number. This figure shows that Fidap 2-D model can work pretty well for low aspect ratio cavities.

4.1.4 Ra=9320, A=20

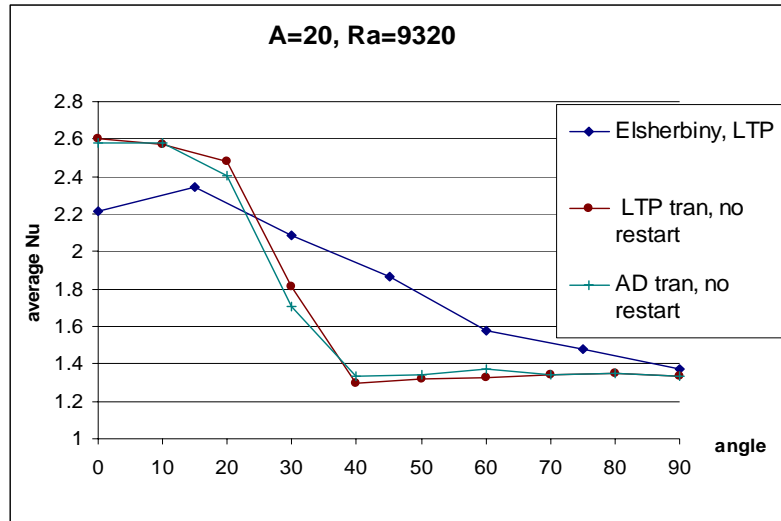


Figure 6: Average Nusselt number from tilt angle 0° to 90° for A=20, Ra=9320.

Figure 6 shows the average Nusselt numbers corresponding to different angle of inclinations together with the experimental data from Elsherbiny et.al. (1982) for the same aspect ratio $A=20$ and $A_z=20$ (the ratio of the depth in z-direction over the width in x-direction) and the same Rayleigh number, using both LTP (linear temperature profile) and AD (adiabatic) boundary conditions for top and bottom walls of the cavity. The LTP was applied in the experimental setup.

As shown above, the 2-D numerical results close to both vertical and horizontal orientations can match the experimental correlations within 15 percent of discrepancy. But the numerical results in the middle angle range can be different from the experimental data up to 30 percent, thus affecting the location of the transition angle. Although 2-D model may be good enough for most design purposes, it is not adequate as a research tool, especially when the accurate location of critical angle is the goal.

4.2 Comparison to published numerical work

Most of the published numerical study on natural convection in inclined enclosures only deals with higher angle of inclination, i.e. the angle range from the transition angle of the flow mode to the vertical orientation. And the choice of the point where they stopped their 2-D calculations was either based on previous study, or based on the point where their 2-D numerical scheme became unstable.

Figure 7 shows the average Nusselt number at different angles from current Fidap 2-D transient calculation compared to some other numerical results (Chen et al [1985], Kuyper et al. [1992] and Zhong et al.[1985]). Figure 8 shows the case for $A=4$, $Ra=3000$ compared with the results from Soong, et.al. (1996). Good agreement from these figures can prove that the current 2-D numerical method is correct in the aspects of mathematical model and the numerical discretization.

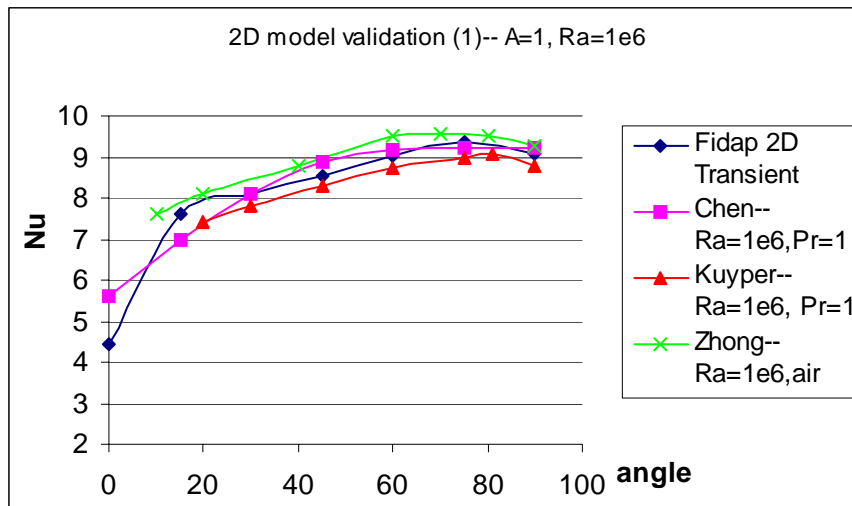


Figure 7: Average Nusselt number from tilt angle 0° to 90° for $A=1$, $Ra=10^6$.

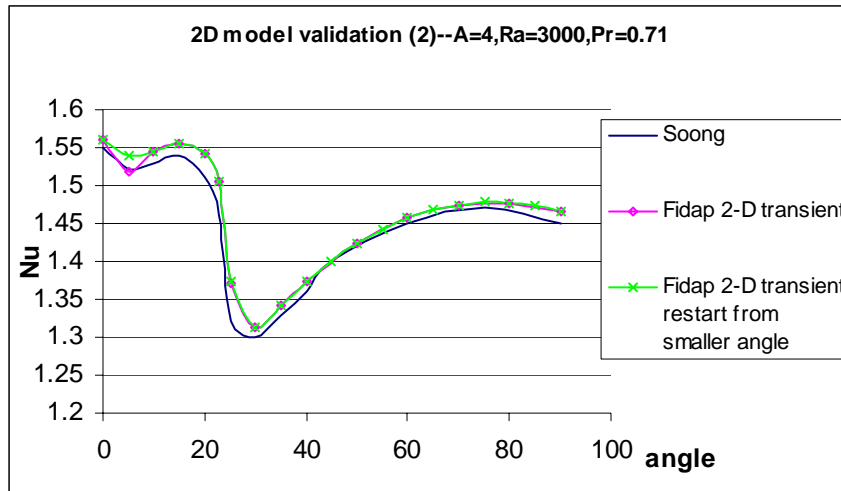


Figure 8: Average Nusselt number from tilt angle 0° to 90° for A=4, Ra=3000.

4.3 Imperfect Boundary Condition Model

4.3.1 Validation of Imperfect Boundary Condition

From the discussion above, it seems that there always exists a mismatch between the experimental results and the 2-D numerical results. According Soong (1996), it is believed that difficulties in control of isothermal wall condition maybe a major reason for the inconsistency. In his study, the perfect constant cold wall temperature was replaced by a weak linear distribution $\Theta^* = \varepsilon(1 - 2y^*/A)$, where ε denotes a perturbation parameter for the imperfection of wall-temperature uniformity.

Figure 9 shows the average Nusselt number results for the same model by current numerical work. Perturbation $\varepsilon = 0.005$ was applied to cold wall temperature distribution, and the results agree quite well with those from Soong et.al. (1996) with the perturbation $\varepsilon = 0.0005$. The prediction of the change-over point of flow pattern occurs at the inclination angle between 5° and 6°, which agrees well with the experimental data, although the peak values are different which is caused by the 3-D effect. It is pointed out

in Soong et.al (1996) that the computed Nu peak is sharper than the measured data, and it is believed that the sharpness stems from the two-dimensionality of the computational model. In addition, there is no significant difference between the Nusselt number for $\varepsilon = 0.005$ and $\varepsilon = 0.0005$. It implies that if the boundary condition is no longer perfect, then the different small disturbances result in negligible changes in heat transfer rate.

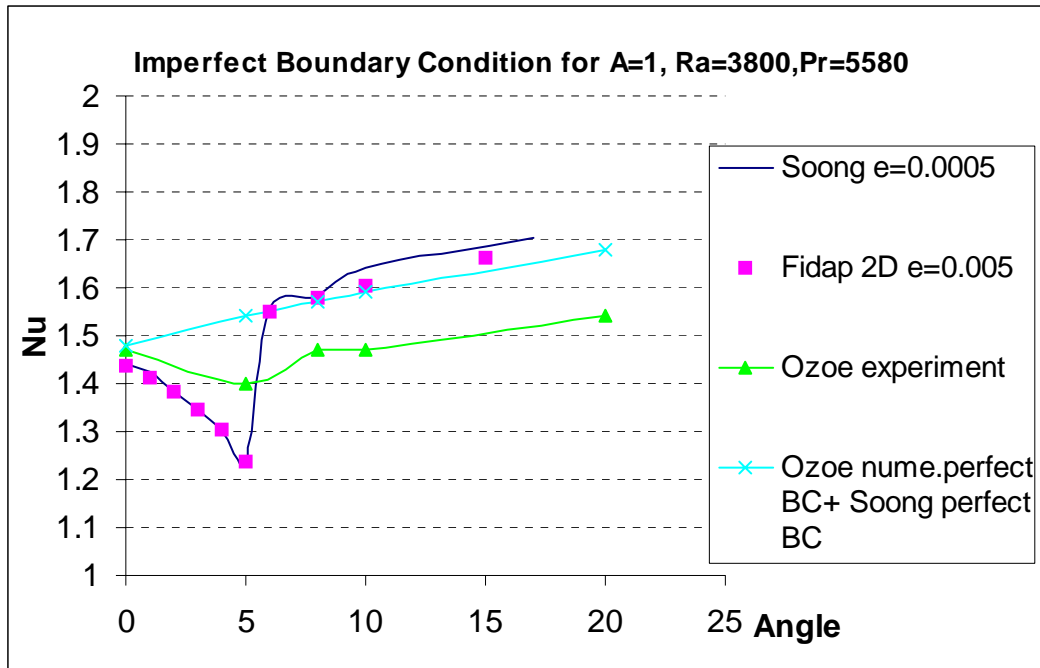


Figure 9: Average Nusselt number for $A=1$, $Ra=3800$, $Pr=5580$ imperfect boundary condition model.

Streamlines and isotherms results from Fidap model at 0° , 5° and 6° with $\varepsilon = 0.005$ are listed in Figure 10 to show the roll of the imperfect boundary condition in this problem. In the perfect case of $\varepsilon = 0$, the cell rotates in counter-clockwise direction. However, in the case of imperfect boundary condition with perturbation factor ε , the difference of the temperature along the cold wall alters the rotating sense of the cell to clockwise. For the cases from 0° to 5° , the upslope shear flow due to buoyancy produces a counter effect on the clockwise rotation of the cell, and the heat transfer decreased. At

6°, the counter effect is large enough to reverse the rotational sense of the cellular motion back to counter-clockwise, which triggers the change of the flow pattern.

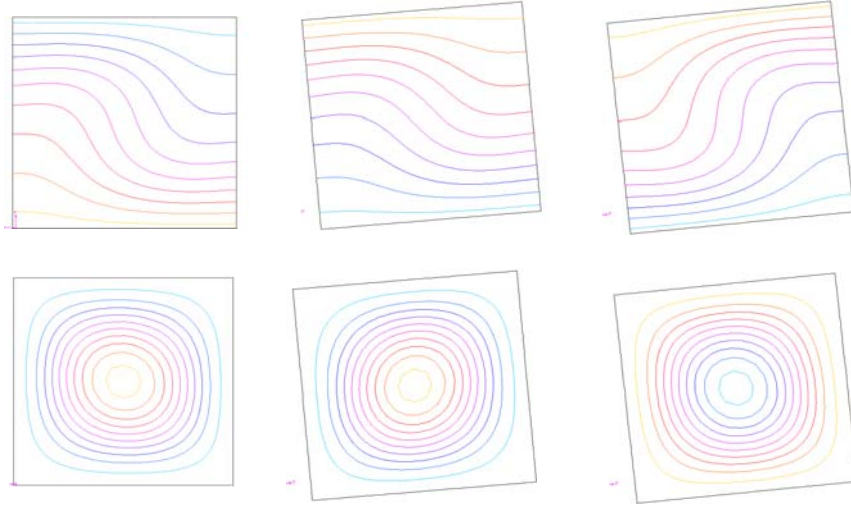


Figure 10. Temperature and Streamline Contours of the cavity with perturbation $\varepsilon = 0.005$, from left to right are 0°, 5° and 6°.

4.3.2 2-D Imperfect Boundary Condition Applications in Fidap Models

This imperfect boundary condition model was applied to one case from Elsherbiny et al (1982), a cavity with aspect ratio 20 and Rayleigh number 9320. Six types of different imperfect boundary conditions were used, which are shown in Table 1.

Table 1. Types of imperfect boundary conditions

Type	Temperature Distributions	
	Cold Wall	Hot Wall
<i>IMBC1</i>	$\theta^*=0.001*(1-2y/A)$	$\theta^*=1.001-0.001*2y/A$
<i>IMBC1a</i>	$\theta^*=0.001*(1-2y/A)$	$\theta^*=1$
<i>IMBC1b</i>	$\theta^*=0$	$\theta^*=1.001-0.001*2y/A$
<i>IMBC2</i>	$\theta^*=0.025*(1-2y/A)$	$\theta^*=1.025-0.025*2y/A$
<i>IMBC2a</i>	$\theta^*=0.025*(1-2y/A)$	$\theta^*=1$
<i>IMBC2b</i>	$\theta^*=0$	$\theta^*=1.025-0.025*2y/A$

Among these types, IMBC1 series correspond to the possible actual minimum temperature deflection of 0.02K, while IMBC2 series correspond to the possible actual maximum temperature deflection of 0.5K in the real experimental setups. Results were shown in Figure 11 together with that of perfect constant wall temperature model, in which there is a zoom-in for the angle range from 55° to 90°. There is obviously not much effect from the temperature deflection model. Considering that the aspect ratio of the cavity analyzed by Soong(1996) is quite small, it is not surprising to have the discrepancy for large-aspect-ratio cavities, even though imperfect boundary conditions have been applied to counter the adverse conditions in the real experiment setup. It can be inferred that the method of imperfect thermal boundary condition is not the real reason to have caused the discrepancy.

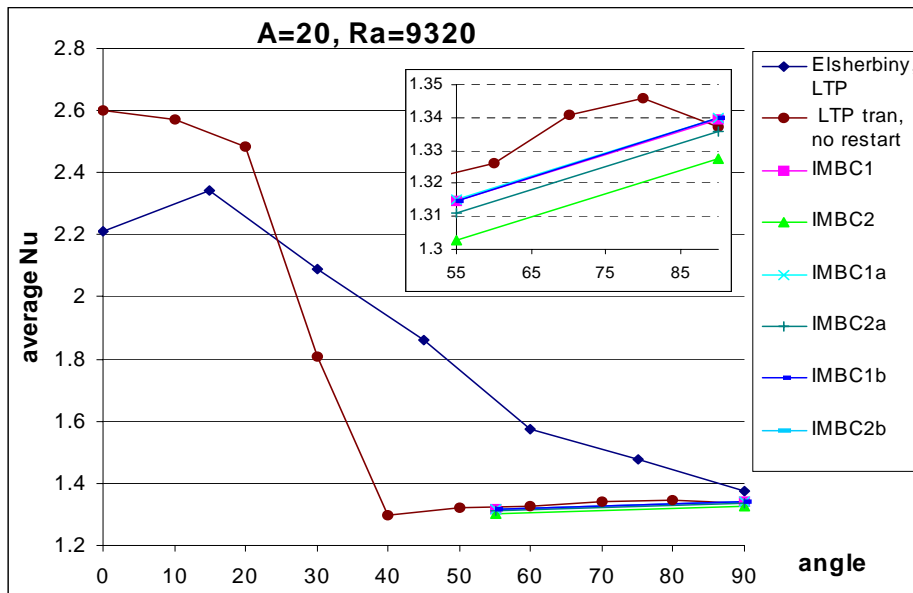


Figure 11. Average Nusselt number Results from Imperfect Boundary Condition Models

4.4 Periodic Temperature Boundary Condition Model

In Elsherbiny et al (1982)'s experimental setup, three electrically heated "heater plates" were imbedded into three recesses machined into the main part of the hot plate to measure flux. Thus, a periodic temperature distribution instead of the constant hot side temperature, was used at the hot side wall to simulate the possible effect from these heat flux meters. The relation used was $\theta^* = 1 - 0.025 \cos(3\pi/10y)$, which is shown in Figure 12. The results were shown in Figure 13, on which the results from the experiment, from the current numerical modeling with perfect boundary condition and with periodic boundary condition on hot wall where compared. However, no effect from the three heat flux meters could be seen.

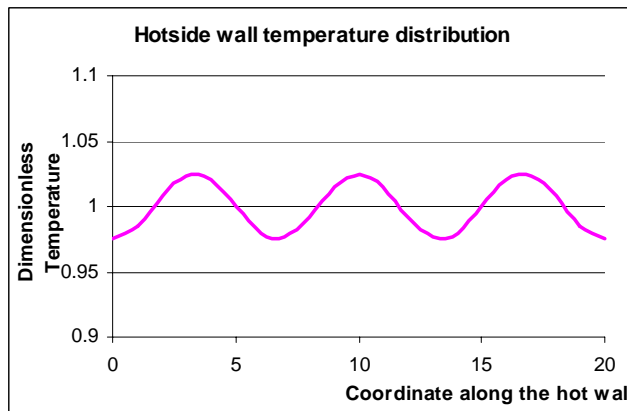


Figure 12. Three Heat Flux Meter Models

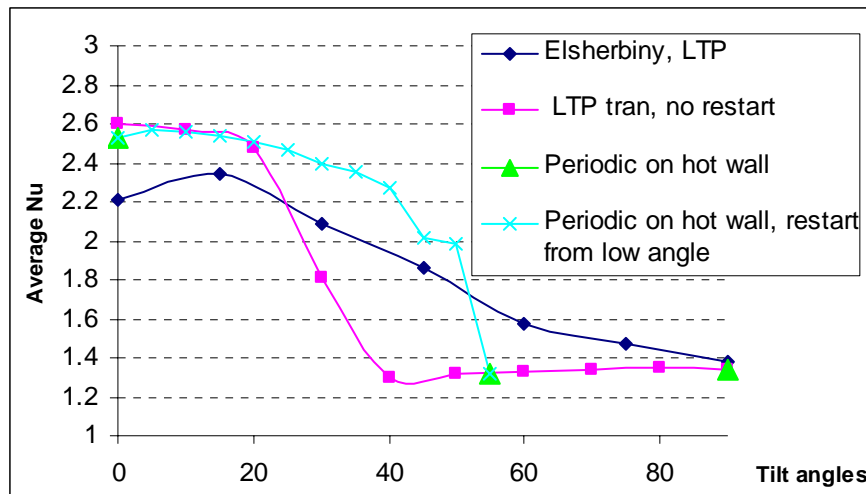


Figure 13. Average Nusselt Number Results from Three Heat Flux Meter Models

4.5 Time-dependent Boundary Condition Model

All the previous discussions were based on time-independent boundary conditions. Here, two types of time-dependent boundary condition models were proposed and simulations based on them were performed. One is the linear increasing temperature at the hot sidewall, which is to simulate the heating process in the real experiment. The other type is that the cold side temperature changes periodically with time, which is to simulate feedback on-ff temperature control method used in the experiment on the cold side. The temperature changing with time for both types was shown in Figure 14 and Figure 15, respectively. The average Nusselt number Nu results also appear time-dependently, which were shown in Figure 16 and Figure 17. The mean values of average Nusselt number over a certain time period were shown in Figure 18.

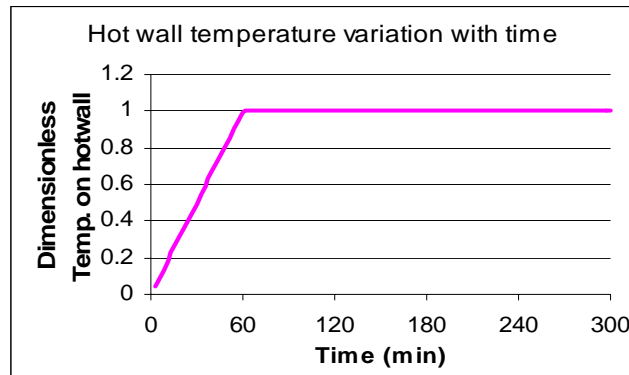


Figure 14. Linear Time-dependent Boundary Condition at the Hot Wall

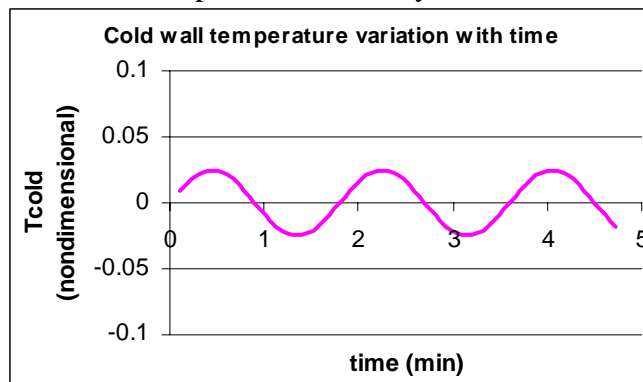


Figure 15. Periodic Time-dependent Boundary Condition at the Cold Wall

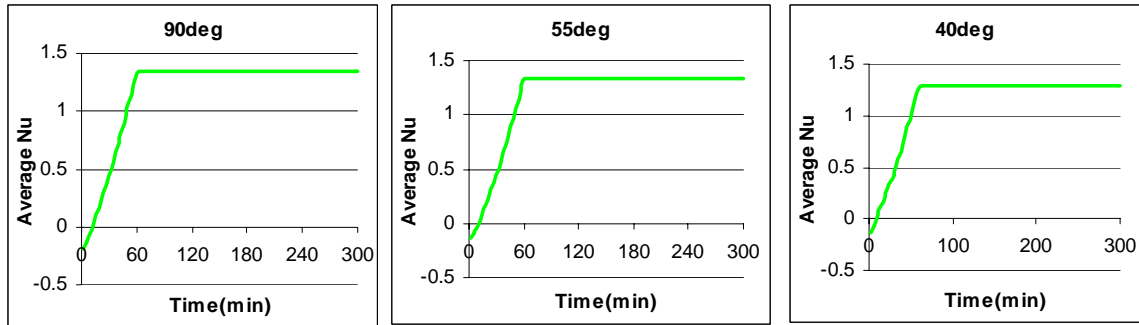


Figure 16. Average Nusselt number Results changing as time for Linear Time-dependent Boundary Condition at the Hot Wall

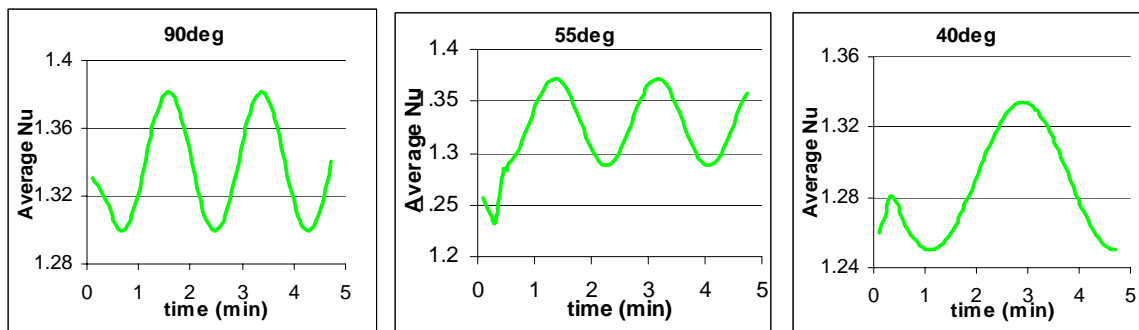


Figure 17. Average Nusselt number Results changing as time for Linear Time-dependent Boundary Condition at the Hot Wall

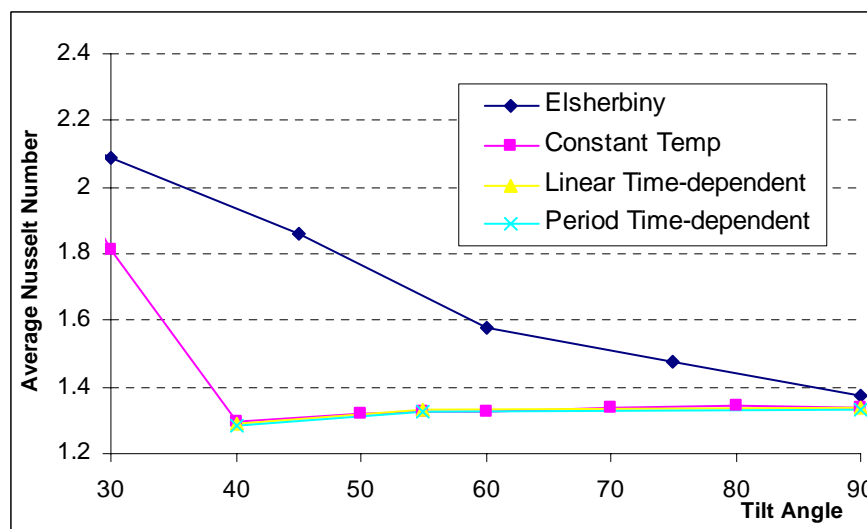


Figure 18. Mean Value over Time of Average Nusselt number Results for Time-dependent Boundary Conditions

Based on Figure 18, not much difference can be found between the results of constant temperature boundary condition and time-dependent boundary condition. A maximum 30 percent relative error can be found at tilt angle around 40° . So up to now, almost all the possible thermal boundary conditions have been proposed and tested and none of them could lead to a successful prediction. At this point, it is believed by the author that three-dimensionality of the flow is the real cause for the discrepancy.

5. Discussions and Future Work

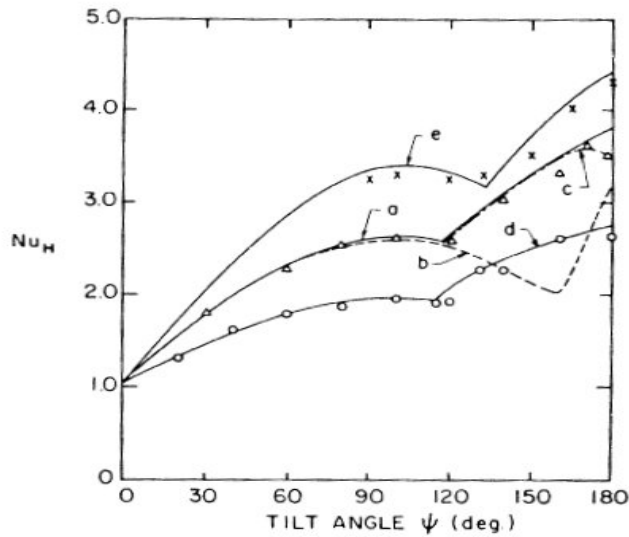
Two-dimensional numerical modeling is an economical and correct way to study natural convection flow in a vertical cavity. However, as the cavity is inclined, especially when the cavity is rotated to smaller tilt angles, two-dimensional model no longer provides heat transfer results, which can match those from experimental work, though comparisons with other 2-D numerical results show that the current 2-D Fidap model is correct in the aspect of mathematical method and its discretization. This mismatch between the obtained numerical results and experimental results are too obvious to be ignored, especially in the middle range of tilt angle. Soong et.al. (1996) proposed two reasons for this mismatch. One is 3-D effect existing in the real flow and the other is imperfect thermal boundary condition in the experimental setup.

Several 2-D numerical models with different thermal boundary conditions were carried out, including non-constant temperature distribution, and time-dependent boundary conditions. However, none of them can provide the same transition point of the flow mode, nor the heat transfer results, as the experimental data. This shows that the 3-D effect is probably the reason which affect the position of the transitional point of the flow mode in the cavity, in turn, affecting heat transfer results.

In Yang H. Q. et al (1986), a two-dimensional model, a three-dimensional “cell” model which was first proposed by Ozoe et al (1983), and a three-dimensional whole cavity model were studied by finite-difference calculations. The cases studied were summarized in Table 2. The average Nusselt number results from the three numerical models are shown in Figure 19. In their study, tile angle ψ is defined as the angle made by the cold wall and the horizontal. As can be seen from Figure 19, 3-D Model provided very close results to the experimental data over the whole angle range; while 3-D Cell Model also could get very close results to experimental data, except a little deflection near the heated-from-below situation. However, 2-D Model started to deflect from the experimental curve beyond the tile angle $\psi = 120^\circ$. In addition, though the same case hasn't been performed in Fidap 2-D simulation, the general characteristics of the average Nusselt number curves from current Fidap modeling also showed the same behavior as that of this work reviewed here.

Table 2. Cases studied in Yang H. Q. et al (1986)

Case	Ra	Geometry	Boundary Conditions at top-bottom walls
1	37150	1x8.4x8.4	Insulated
2	12350	1x8.4x8.4	Insulated
3	80000	1x5.0x5.0	Perfectly Conducting



Case	Exp.
1	Δ
2	o
3	x

Figure 19. Average Nusselt Number Results from H. Q. Yang (?): 3-D Cell Model curve a (Case 1), curve d (Case 2), curve e (Case 3); 2-D Model curve b (Case 1); 3-D Whole Cavity Model curve c (Case 1).

Thus, three-dimensional modeling is promising to get close results to those of experimental work. Both 3-D cell model and 3-D whole cavity model could be chosen as the modeling method. 3-D cell model is probably the more economical way to save computational resource and time, but the difficulty relies in that the cell width is an unknown parameter which needs further study, plus there is a little bit of mismatch at the very small tilt angle. 3-D whole cavity model would provide more accurate results, costing more computational time.

So, in the next stage of this research work, 3-D modeling will be applied to solve the problem of fluid flow and heat transfer inside the inclined cavities. Both 3-D whole cavity model and 3-D cell model will be used to study the problem. The former method

will concentrate on studying the physics of this type of flow and heat transfer. Insight gained from the whole cavity model can help to identify the important parameter in the 3-D cell model – cell width. The latter method will be applied to generate a significant amount of data about the fluid flow and heat transfer inside the cavity because it is more time-efficient. Based on the data obtained, further study can extract very valuable information concerning about the phenomena inside the cavity, such as the dependence of critical angle on aspect ratio and relationship between Nusselt number and aspect ratio, as well as Rayleigh number, under a certain tilt angle. So the research in next stage will be yielding very valuable information for the designing of fenestration system.

Reference:

- Arnold, J.N., I. Catton and D.K.Edwards. 1976. Experimental Investigation of Natural Convection in Inclined Rectangular Regions of Differing Aspect Ratios. *Journal of Heat Transfer*. Vol. 98, pp.67-71.
- Catton, I., P.S., Ayyaswamy and R.M., Clever, 1974. Natural Convection Flow in a Finite, Rectangular Slot Arbitrarily Oriented with respect to the Gravity Vector. *International Journal of Heat and Mass Transfer*, Vol. 17, pp.173-184.
- Chen, C.J. and V. Talaie. Finite Analytic Numerical Solutions of Laminar Natural Convection in Two-Dimensional Inclined Rectangular Enclosures. *ASME paper 85-HT-10*. 1985.
- Elsherbiny, S.M., G.D. Raithby, K.G.T. Hollands. 1982. Heat Transfer by Natural Convection across Vertical and Incline Air Layers. *Transactions of the ASME*. 96/ Vol. 104, Feb.
- Hamady, F. J., H. R. Lloyd, H. Q. Yang and K. T. Yang. 1989. Study of Local Natural convection Heat Transfer in an Inclined Enclosure. *International Journal of Heat and Mass Transfer*. Vol. 32,pp.1697-1708.
- Hollands, K.G.T., L.Konicek. 1973. Experimental Study of the Stability of Differentially Heated Inclined Air Layers. *International Journal of Heat and Mass Transfer*. Vol. 16,pp.1467-1476.

- Kuyper, R.A., Th. H. Van Der Meer, C. J. Hoogendoorn and R. A. W. M. Henkes. 1992. Numerical Study of Laminar and Turbulent Natural Convection in an Inclined Square Cavity. *International Journal of Heat and Mass Transfer*, Vol. 36, No. 11, pp. 2899-2911.
- Linthorst, S.J.M., W.M.M.Schinkel , C.J.Hoogendorn. 1981. Flow Structure with Natural convection in Inclined Air-filled Enclosures. *Journal of Heat Transfer*. Vol. 103, pp.535-539.
- Ozoe, H. H. Sayama and S. W. Churchill. 1974a. Natural Convection in an Inclined Square Channel. *International Journal of Heat and Mass Transfer*. Vol. 17,pp.401-406.
- Ozoe, H., K., Yamamoto, H., Sayama and S. W. Churchill. 1974b. Natural Circulation in an Inclined Rectangular channel heated on One Side and cooled on the Opposing side. *International Journal of Heat and Mass Transfer*. Vol. 17,pp.1209-1217.
- Ozoe, H., H. Sayama and S. W. Churchill. 1975. Natural Circulation in an Inclined Rectangular channel at Various Aspect Ratios and Angles—experimental Measurements. *International Journal of Heat and Mass Transfer*. Vol. 18,pp.1425-1420.
- Ozoe, H., H., Sayama and S. W. Churchill. 1977. Natural Convection Patterns in a Long Inclined Rectangular Box Heated From Below—1. Three-directional Photography. *International Journal of Heat and Mass Transfer*, v 20, n 2, Feb, 1977, pp 123-129.
- Ozoe, H. and K. Fujii. 1983. Long Rolls Generated by Natural Convection in an Inclined, Rectangular Enclosure. *International Journal of Heat and Mass Transfer*, v 26, n 10, Oct, 1983, pp 1427-1438.
- Schinkel , W.M.M., C.J.Hoogendorn. 1978. An Interferometric Study of the Local Heat transfer by Natural convection in Inclined Airfilled Enclosures. *Proceedings of the 6th Int. Heat Transfer Conference*. Toronto.Vol 2, pp. 287-292
- Soong, C. Y., P. Y. Tzeng, D. C. Chiang and T. S. Sheu. 1996. Numerical Study on Mode-transition of Natural Convection in Differentially Heated Inclined Enclosures. *International Journal of Heat and Mass Transfer*. Vol. 39, No. 14, pp.2869-2882.
- Yang, H. Q., K. T. Yang and J. D. Lloyd. 1986. Flow Transition in Laminar Buoyant Flow in a Three-dimensional Tilted Rectangular Enclosure. *Proceedings of the International Heat Transfer Conference*, v 4, 1986.
- Zhong, Z.Y., K.T. Yang and J.R. Lloyd. 1985. Variable-property Natural convection in tilted Enclosures with Thermal Radiation. *Numerical Methods in Heat Transfer*. Vol. III, pp. 195-214.